Mo gapping in 3 BO_3 pero ki e i ho Mo -H bbard in erelec ronic rep l ion enerG U

Julien Varignon,[1] Manuel Bibes,[1] and Alex Zunger[2]
[1]*Unité Mixte de Physique, CNRS, Thales, Université Paris Sud, Université Paris-Saclay, 91767, France*
[2]*Energy Institute, University of Colorado, Boulder, Colorado 80309, USA*

shellshas + U represents interelectronic correlation be the approa wa ad em pi the H Hamiltonian, and if empiricism in selecting U can be avoided. Here we illustrate that *ab initio* DFT *any* U is able to predict gapping trends and structural symmetry breaking (octahedra rotations, Jahn modes, bond disproportionation) for all 3*d ABO*

$_3$ perovskites from titanates to nickelates in both spin-ordered and spin-disordered paramagnetic phases. Thus, the mechanism of gap formation due to the Hubbard Hamiltonian dynamic interelectronic correlation is not a requirement in these 3*d* electron compounds. We describe the paramagnetic phases as a supercell where individual sites can have different local environments thereby allowing DFT to develop finite moments on different sites as long as the total cell has zero moment. We use the recently developed strongly constrained appropriately normed exchange and correlation functional (SCAN) that is sanctioned by the usual single-determinant, mean-field DFT paradigm with static correlations, but has a more precise rendering of self-interaction cancelation. Our results suggest that strong dynamic electronic correlations are not playing a universal role in gapping of 3*d* ABO_3 Mott insulators, and opens the way for future applications of DFT for studying a plethora of complexity effects that depend on the existence of gaps, such as doping, defects, and band alignment in ABO_3 oxides.

DOI: 10.1103/PhysRevB.100.035119

ABO

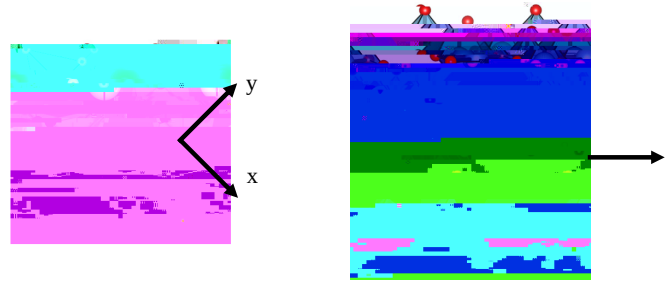
y
x

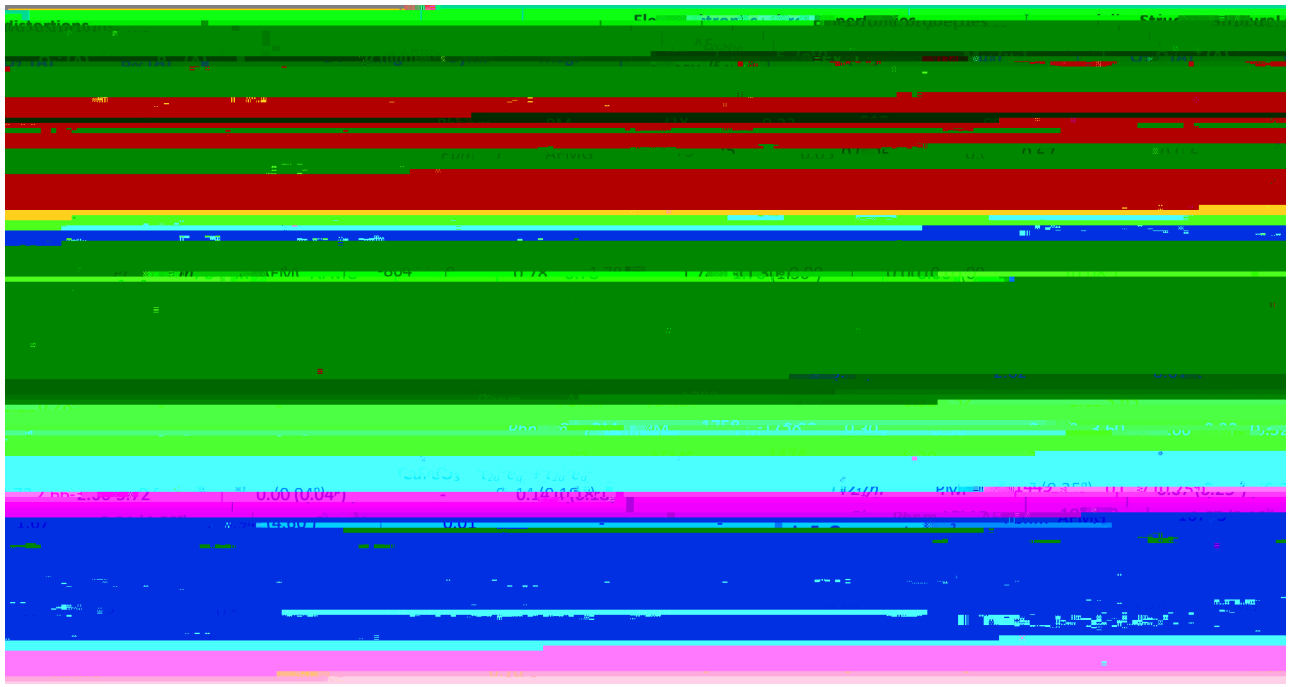

FIG. 2. Key properties of oxide perovskites with the SCAN meta-GGA functional without U. We use the SQS supercell for the PM phase. ΔE_{NM} (meV/f u) is the energy difference between the current spin polarized and the Naive DFT (N-DFT) solution. E_g is the band gap (in eV), M_{3d} is the local moment (in μ_{B}) associated with the B cation. Q_2^-, Q_2^+ and B_{oc} are the octahedral deformation amplitudes (in Å) (experimental values are provided in parenthesis). Ins. stands for insulating phases. Experimental values are taken from a: Ref. [40], b: Ref. [41], c: Ref. [42], d: Ref. [43], e: Ref. [44], f: Ref. [45]; g: Ref. [46], h: Ref. [47], i: Ref. [48], j: Ref. [49], k: Ref. [50], l: Ref. [51], m: Ref. [52], n: Ref. [53], o: Ref. [54], p: Ref. [5], q: Ref. [55], r: Ref. [56], s: Ref. [57], t: Ref. [58], u: Ref. [4], v: Ref. [59], w: Ref. [60].

moment $M_{3\mathrm{d}}$ (in μ_{B}) associated with the B cations and amplitudes of distortions (in Å) associated with $Q_2{}^+$, $Q_2{}^-$ and bond disproportionation motions, all done without Hubbard U, compared with experimental values available in literature. The calculated energy-minimizing lattice type agrees with experiments with the exception of YVO_3 and $LaVO_3$ in the PM phase and $CaFeO_3$ in the AFM phase. In the two vanadates, the strongly entangled spin and orbital degrees of freedom induce small lattice distortions on each octahedra in the PM phase (where each transition metal element experiences a unique potential), thus reducing the symmetry from $P2_1/c$ to P-1 [38]. However, the lattice parameters, B-O-B angles and B-O bond lengths are very similar to the respective quantities observed in experimental structures. For $CaFeO_3$, the AFM-S magnetic order that we have used to approximate the experimentally observed AFM spiral [5] breaks the inversion center and induces some small lattice distortions such as polar displacements [39], thus producing a polar $P2_1$ space group instead of a centrosymmetric $P2_1/n$ symmetry.

Band gaps without U. All ABO_3 compounds tested here are insulators in both their spin-ordered and spin-disordered PM solutions (Fig. 2). These results agree with the insulating character observed experimentally (some experimental values available in literature are reported in Fig. 2) and also reproduce trends observed with DFT+U and DMFT simulations on some of these materials (e.g.,$R\mathrm{TiO}_3$, $R\mathrm{VO}_3$, $R\mathrm{MnO}_3$ and $R\mathrm{NiO}_3$, see references therein). For instance, we observe insulation in the yttrium nickelate $YNiO_3$ compound in both AFM and PM phases, as DMFT does in the $LuNiO_3$ PM phase [14,61]. Likewise, we also observe an increase in the band gap when going from rare-earth titanates (d^1) to rare-earth vanadates (d^2) in agreement with experimental observations [41,45]. We emphasize here that experimental data of structural and electronic properties on bulk and stoichiometric $LaCuO_3$ crystals are scarce and diverging hindering confirmation of the SCAN-DFT calculation. Finally, just as standard exchange and correlation functionals underestimate the band gap of the highly uncorrelated semiconductors such as Si and GaAs, the SCAN functional behaves similarly for ABO_3 materials and one may improve the band gap description and related quantities by using GW corrections [62].

Magnetic moments. Our calculations provide magnetic moment values that are comparable to experimental quantities available in literature (see Fig. 2). For instance, we capture the decrease of the magnetic moment of Ti cations when going from $YTiO_3$ to $LaTiO_3$ [40,43]. Due to the presence of a double local environment (DLE) for Ni and Fe cations in $YNiO_3$ and $CaFeO_3$, respectively, two very different magnetic moments are extracted from our simulations. These quantities, compatible with experimental values, point towards a disproportionation of the unstable 3+ and 4+ formal oxidation states (FOS) of Ni and Fe cations, respectively, towards their more stable 2+/4+ and 3+/5+ FOS.

Trends in energy differences between different phases. The energy gain in forming local moments is given by the total energy difference E_{NM}-E_{AFM}. As the number of unpaired 3*d* electrons increases, we see that this energy strongly increases, signaling the large energy gain obtained by forming local

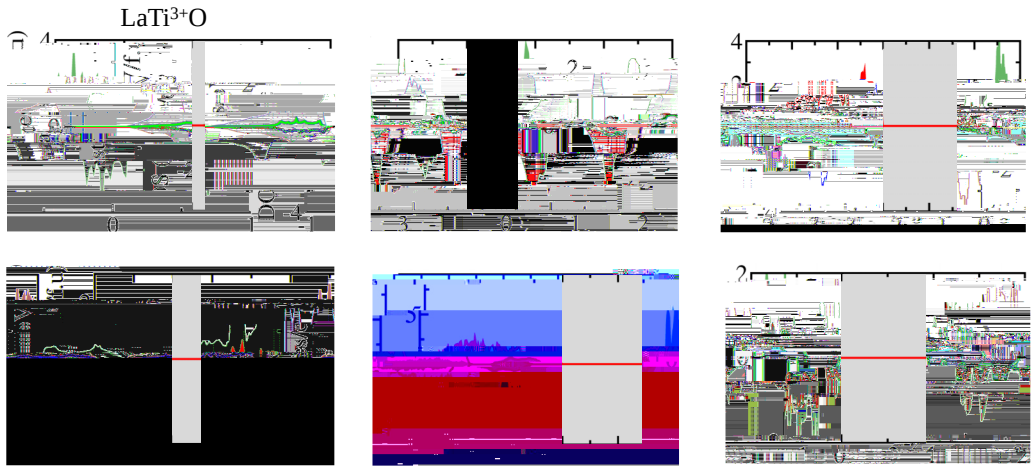
LaTi3+O

[1] D. I. Khomskii, *Transition Metal Compounds* (Cambridge University Press, Cambridge, 2014).
[2] S. Miyasaka, Y. Okimoto, M. Iwama, and Y. Tokura, Phys. Rev. B **68**, 100406(R) (2003).
[3] X. Qiu, T. Proffen, J. F. Mitchell, and S. J. L. Billinge, Phys. Rev. Lett. **94**, 177203 (2005).
[4] J. A. Alonso, J. L. García-Muñoz, M. T. Fernández-Díaz, M. A. G. Aranda, M. J. Martínez-Lope, and M. T. Casais, Phys. Rev. Lett. **82**, 3871 (1999).
[5] P. M. Woodward, D. E. Cox, E. Moshopoulou, A. W. Sleight, and S. Morimoto, Phys. Rev. B **62**, 844 (2000).
[6] N. F. Mott and Z. Zinamon, Rep. Prog. Phys. **33**, 881 (1970).
[7] N. Mott, *Metal-Insulator Transitions* (CRC Press, Boca Raton, FL, 1990).
[8] J. Hubbard, Proc. R. Soc. A Math. Phys. Eng. Sci. **276**, 238 (1963).
[9] J. Hubbard, Proc. R. Soc. London Ser. A **281**, 401 (1964).
[10] R. E. Cohen, Nature (London) **358**, 136 (1992).
[11] G. Pacchioni, J. Chem. Phys. **128**, 182505 (2008).
[12] F. Lin, I. M. Markus, D. Nordlund, T.-C. Weng, M. D. Asta,

[60] J. A. Alonso, M. J. Martínez-Lope, M. T. Casais, M. A. G. Aranda, and M. T. Fernández-Díaz, J. Am. Chem. Soc. **121**, 4754 (1999).
[61] A. Hampel, P. Liu, C. Franchini, and C. Ederer, npj Quantum Mater. **4**, 5 (2019).
[62] F. Giustino, Rev. Mod. Phys. **89**, 015003 (2017).